Journal of Fluorescence
https://doi.org/10.1007/s10895-025-04259-1

RESEARCH

Detection of Trace Amounts of Fe^{3+} and Cr^{6+} Ions Using a ZIF-8 Fluorescent Sensor with High Selectivity and Fast Response

Fariba Erfani Jazi[1] · Sayed Mehdi Ghoreishi[1] · Ali Gholami[1]

Received: 29 November 2024 / Accepted: 9 March 2025

Abstract

While zeolitic imidazole framework (ZIF)-based materials have shown promising metal ion detection performances, they did not achieve the same results as for pure ZIFs. Here, a highly porous ZIF-8 material is synthesized using a chemical method under stirring at room temperature, and characterized in terms of crystallinity and chemical state. The resulting ZIF-8 is employed as a multifunctional fluorescent sensor to detect Fe^{3+} and Cr^{6+} metal ions dissolved in water, exhibiting high luminescence with a broad wavelength band in the visible light region. The water-soluble metal ions are found to be very sensitive to a decrease in the luminescence intensity of ZIF-8, and can be detected at trace amounts with high selectivity. The detection limits of Fe^{3+} and Cr^{6+} ions are achieved to be 2.1×10^{-6} and 7.6×10^{-7} M, respectively. The intensity of luminescence decreases with increasing the concentration of both metal ions, thereby giving rise to the complete fluo>rescence quenching with a very fast response time using Fe^{3+} and Cr^{6+} ion concentrations higher than 1.0×10^{-4} and 4.7×10^{-5} M, respectively. These results may pave the way for the utilization of pure ZIF materials in the development of highly efficient fluorescent sensors in order to rapidly detect trace amounts of environmental pollutants.

Highlights

- A hydrothermal method is used to synthesize pure ZIF-8 with high porosity and crystallinity.
- The synthesized ZIF is utilized as a multifunctional fluorescent sensor to detect various metal ions.
- The pure ZIF-based sensor shows detection limits of 2.1 and 0.76 µM for Fe^{3+} and Cr^{6+} ions, respectively.
- The intensity of luminescence decreases with increasing the concentration of Fe^{3+} and Cr^{6+} ions.
- Fe^{3+} and Cr^{6+} quenching occurs by the resonance energy transfer and collapse of ZIF-8 main framework, respectively.

Keywords Metal–organic framework · ZIF-8 · Photoluminescence spectrometry · Fluorescent sensor · Metal ion detection

Introduction

Interest in recognition and detection of metal ions continues its upward trajectory because of their link to both the human health and the environment. The occurrence of several diseases, including sleep disorders, anemia, liver damage and heart failure as well as fatal illnesses (e.g., cancer) can be increased due to the presence of different heavy metals ions, particularly those that exceed the allowed concentration limits. As a result, it is vital to detect and measure the concentration of metal ions that might be harmful to humans and other living organisms [1–3].

The presence of some metal ions (e.g., iron (Fe^{3+}) and hexavalent chromium ($Cr_2O_7^{2-}$ and CrO_4^{2-})) in industrial and agricultural wastewaters has considerably raised fears and concerns [2]. As an essential metal ion for most organisms, Fe^{3+} ion plays a significant role in biochemical processes, involving the oxygen transport, cellular metabolism, nitrogen stabilization, oxygen conduction, and electron transport in DNA and RNA synthesis [2, 4–6]. Moreover, the structure and activity of enzymes and proteins can be maintained and controlled through Fe^{3+} ions. Consequently, raising or lowering the Fe^{3+} ion level can lead to a number of diseases, including insomnia, heart failure, pancreas,

✉ Sayed Mehdi Ghoreishi
s.m.ghoreishi@kashanu.ac.ir

[1] Department of Analytical Chemistry, Faculty of Chemistry, University of Kashan, P.O. Box 87317-51167, Kashan, Islamic Republic of Iran

Published online: 23 April 2025

Parkinson's, Alzheimer's, liver damage, agrypnia, arthritis, iron deficiency anemia, coryza, cancer, etc. [3, 5–7].

Because of its high stability and ability to cause cancer even at extremely small concentrations, Cr^{6+} ion has been proposed by the World Health Organization (WHO) as one of the most dangerous water-soluble heavy metal pollutants, being considered a serious threat to human and aquatic life. For this reason, the detection of trace amounts of Cr^{6+} ion has been extensively studied and demanded [8–10]. It is known that chromium exists in the form of chromate (CrO_4^{2-}) and dichromate ($Cr_2O_7^{2-}$) ions with long-term stability in water, soil and air, being a crucial oxidant in laboratory and industrial applications. Nevertheless, the toxicity of chromium is manifold and can give rise to different kinds of cancer, allergic reactions, and and genetic defects due to its strong mutagenicity and carcinogenicity [10, 11]. Generally, industries such as production of leather tanning, textile manufacturing, steel fabrication and so forth are major sources of Cr^{6+} contaminants [11]. In order to monitor and protect the environment, it is imperative to rapidly and reliably detect water-soluble Cr^{6+} ions [2].

Metal–organic frameworks (MOFs) with unique properties are a class of inorganic–organic hybrid materials, having coordination bonds connecting metal centers and organic linkages, and forming a large family of one-, two-, or three-dimensional crystalline solids. [1, 5, 13]. The term "MOF" was first introduced by Yaghi in 1995 [5]. The chemical structure of the metals and ligands affects physical and chemical properties of MOFs. The designable structure, modifiable pore surface, numerous adsorption sites, and target-specific host–guest interaction are among the advantages of MOFs [1, 5], attracting considerable attention worldwide in the past decades. These frameworks not only have a special crystal structure, but also possess special applications in gas storage and separation, multiphase catalysis, drug delivery, biomedicine, and sensors due to their unique properties such as high thermal and chemical stability, diverse and adjustable topology, tunable porosity, and large specific surface area [1, 14–16].

In general, among different types of frameworks, MOFs with luminescent properties have shown clear superiority, and are more effective and ideal by having higher selectivity and sensitivity, lower detection limit, faster response time, easier operation and low cost in the process of measuring metal ions, organic molecules, explosive compounds, and biological molecules [2, 14, 16, 17]. Therefore, the MOF-based detection method is considered a great alternative to sophisticated techniques such as high-performance liquid chromatography (HPLC), ion chromatography (IC), electrophoresis, inductively coupled plasma optical emission spectroscopy (ICP-OES), ICP mass spectrometry (ICP-MS), emission spectrometry, atomic absorption, and electrochemical methods. [5, 6]. On the other hand, these precise instruments involve intricate and complex procedures, along with complex sample preparation and high cost [2, 3, 8] Basically, the luminescent properties of MOFs can be easily controlled by diverse metal nodes (e.g., lanthanide metal group or transition metals) and guest species [3]. Furthermore, the progress in the field of MOFs based on the luminescent properties offers great opportunities for their applications in medical diagnostics, cell biology, and sensor fabrication [14, 18].

As a subclass of MOFs, zeolitic imidazolate frameworks (ZIFs) have three-dimensional crystalline structures made up of transition metal ions (e.g., Zn (ZIF-8), Co (ZIF-67), and Cu ($Cu(IM)_2$)) that are tetrahedrally coordinated and connected by imidazole or imidazolate type linkers [19]. Among ZIFs, the ZIF-8 consisting of zinc metal bonds and 2-methyl-imidazole (2-MeIm) ligands has been recognized as a leading material for gas storage and separation, multiphase catalysis, drug delivery and heterogeneous catalysis, arising from its high porosity, sodalite morphology, and exceptional chemical and thermal stability.

The charge transfer between MeIm units and Zn^{2+} ions causes ZIF-8 to emit pale blue light [15, 20], therefore also exhibiting luminescence function of host–guest hybrids, which can be utilized in the investigation and development of medical, environmental and industrial applications [20, 21]. So far, many MOFs have been developed for the purpose of identifying metal ions. However, high selectivity and fast response in detecting trace amounts of Fe^{3+} and Cr^{6+} ions by pure ZIF-8 is yet to be achieved. In fact, one of the challenges in the detection of Fe^{3+} ion is its interference with other metal ions such as Cu^{2+}, making it essential to prepare a sensor with high sensitivity without being affected by other ions [4, 12, 21–25]. Also, a large number of MOF-based iron-detecting sensors are limited to the use of organic solvents, thereby severely restricting the utilization of these devices in biological and environmental solutions [12, 21, 26–29].

The purpose of this paper is to detect Fe^{3+} and Cr^{6+} ions in aqueous solutions by using a multi-response fluorescent sensor with simple structure and excellent selectivity and sensitivity. In this regard, a chemical method under stirring at room temperature is used to synthesize pure ZIF-8, followed by characterizing its crystal structure and chemical state. Also, luminescent properties are investigated for the fluorescent sensor mixed with various metal ions such as Al^{3+}, Cr^{3+}, Fe^{3+}, $Cr_2O_7^{2-}$, CrO_4^{2-}, IO_3^-, etc. This study manifests the capability of pure ZIF-8 in the precise and rapid detection of Fe^{3+} and Cr^{6+} metal ions in aqueous medium.

Experimental Details

Materials and Instrumentation

All reagents listed in the following were analytical grade and used without further purification: 2-MeIm, zinc nitrate hexahydrate ($Zn(NO_3)_2 \cdot 6H_2O$), and methanol.

The nitrate and potassium compounds were purchased from Merck company. The crystal structure and phase of ZIF-8 were studied using an X´Pert Pro rotating anode X-ray diffractometer (XRD; Cu-Kα radiation, $\lambda = 1.54$ Å). Rietveld refinement of the measured XRD pattern was performed using Xpert High Score software. Fourier transform infrared spectroscopy (FT-IR) with KBr pellets was used in the range of 400–4000 cm^{-1} by a Tensor 27 spectrometer. The disperse fluorescence spectrum was excited by a xenon lamp and obtained using a Perkin Elmer LS 55 fluorescence spectrophotometer with emission and excitation slit widths of 10 nm. All the measurements were completed under the same conditions [13].

Synthesis of ZIF-8

$Zn(NO_3)_2{\cdot}6H_2O$ (0.879 g) and 2-MeIm (2.673 g) were separately dissolved in 20.0 ml of methanol solution, and then mixed with each other under magnetic stirring (1500 rpm, 5 h) at room temperature, so that a white precipitate was obtained. Afterwards, the precipitate in the solution was centrifuged (10000 rpm, 5 min) and washed three times with methanol. Finally, the resultant precipitate was dried at 80 °C to obtain ZIF-8 powder, and kept in the dark for the subsequent experiments [15].

Fluorescence Measurements of ZIF-8

0.0455 g of ZIF-8 powder was gently ground using a mortar, and then completely dispersed in 20.0 ml of deionized water under ultrasonication in order to prepare a concentration of 0.01 M. The fluorescence spectrum was then measured at the excitation wavelength (λ_{ex}) of 396 nm. It should be noted that the maximum emission wavelength of ZIF-8 was 555 nm. From now on, the ZIF-8 dispersed in the deionized water with a concentration of 0.01 M will be referred to as ZIF-8(a).

Selective Measurement of Different Metal Ions

In order to evaluate the luminescence sensing selectivity of ZIF-8(a), it was added into $M(NO_3)_X$ and $K_X(A)$ solutions, where M represents Al^{3+}, Cr^{3+}, Fe^{3+}, Ni^{2+}, Fe^{2+}, Co^{2+}, Mg^{2+}, Cd^{2+}, Ca^{2+}, Mn^{2+}, Na^{+}, and K^{+}, and A includes $Cr_2O_7^{2-}$, CrO_4^{2-}, IO_3^{-}, SO_4^{2-}, Br^{-}, Cl^{-}, ClO_4^{-}, and NO_3^{-}. In this respect, ZIF-8(a) was mixed with the metal ions (1:1 in ratio) at a concentration of 0.01 M, followed by recording the luminescence spectra of the mixture. It should be noted that the blank sample contained 4.0 ml of ZIF-8(a) suspension.

Results and Discussion

XRD and FT-IR Results

Figure 1(a) shows the XRD pattern of ZIF-8. The peaks positioned at $2\theta = 7.526°$, 10.576°, 12.916°, 14.894°, 16.639°, 18.219°, 22.321°, 24.69°, 25.81°, 26.87° and 29.86 correspond to (011), (002), (112), (022), (310), (222), (114), (233), (134), (044) and (244) crystal planes, respectively. The strong peaks intensity is indicative of an excellent crystal structure, being in good agreement with the sodalite ZIF-8 structure [29]. Moreover, the absence of any other peaks in the XRD pattern suggests that the synthesized ZIF-8 is pure [12, 29–32]. Rietveld refinement of the XRD pattern is also shown in Fig. 1(a), matching well with the measured data. The crystal lattice parameter of the ZIF-8 is calculated to be 17.007 Å in a cubic structure with I −4 3 m space group, being in agreement with the reported value of.

ZIF-8 [33]. Tables S1 and S2 in Supporting Information present more details about the crystal lattice and unit cell parameters calculated from the Rietveld refinement.

The FT-IR spectrum of the ZIF-8 is shown in Fig. 1(b). As observed, the band positioned at 3227 cm^{-1} can be attributed to N–H stretching vibration of 2-MeIm [8, 19]. Noticeably, the Zn-N band stretching vibration appeared around 440 cm^{-1} indicates the formation of imidazolate when zinc ions are chemically combined with the nitrogen atoms of 2-MeIm ligand [34]. The aforementioned band can also be assigned to the rich π system of the imidazole ring [25]. The C-H asymmetric stretching vibrations are observed at 2966 and 3055 cm^{-1} [35]. The strong band positioned around 1573 cm^{-1} is induced by the C=C stretching vibration, and the band at 1421 cm^{-1} is responsible for the C=N stretching vibration [30, 31, 35, 36].

Fluorescence Spectrum of ZIF-8(a)

The excitation and fluorescence emission spectra of ZIF-8(a) are shown in Fig. 2(a) and (b), respectively. The maximum emission intensity of ZIF-8(a) is observed at $\lambda_{ex} = 396$ and 555 nm. Previous studies have indicated that ball-milled ZIF-8 particles show strong solid-state fluorescence emissions at λ_{ex} in the range of 396–450 nm [2, 20, 37]. The peak shift observed in the present study can be attributed to the introduction of the guest species (i.e., water) into the highly crystalline structure of ZIF-8. The strong interactions taking place between the guest and host firmly fix the guest species in ZIF-8. As well, the guest molecules can modulate the frontier orbitals in the host–guest system to a large extent. Compared to ZIF-8 powder, ZIF-8(a) has a longer emission wavelength and a lower energy gap, which can reasonably correspond to the significant emission changes in the spectrum [38]. In addition, the surface adsorption of solvent

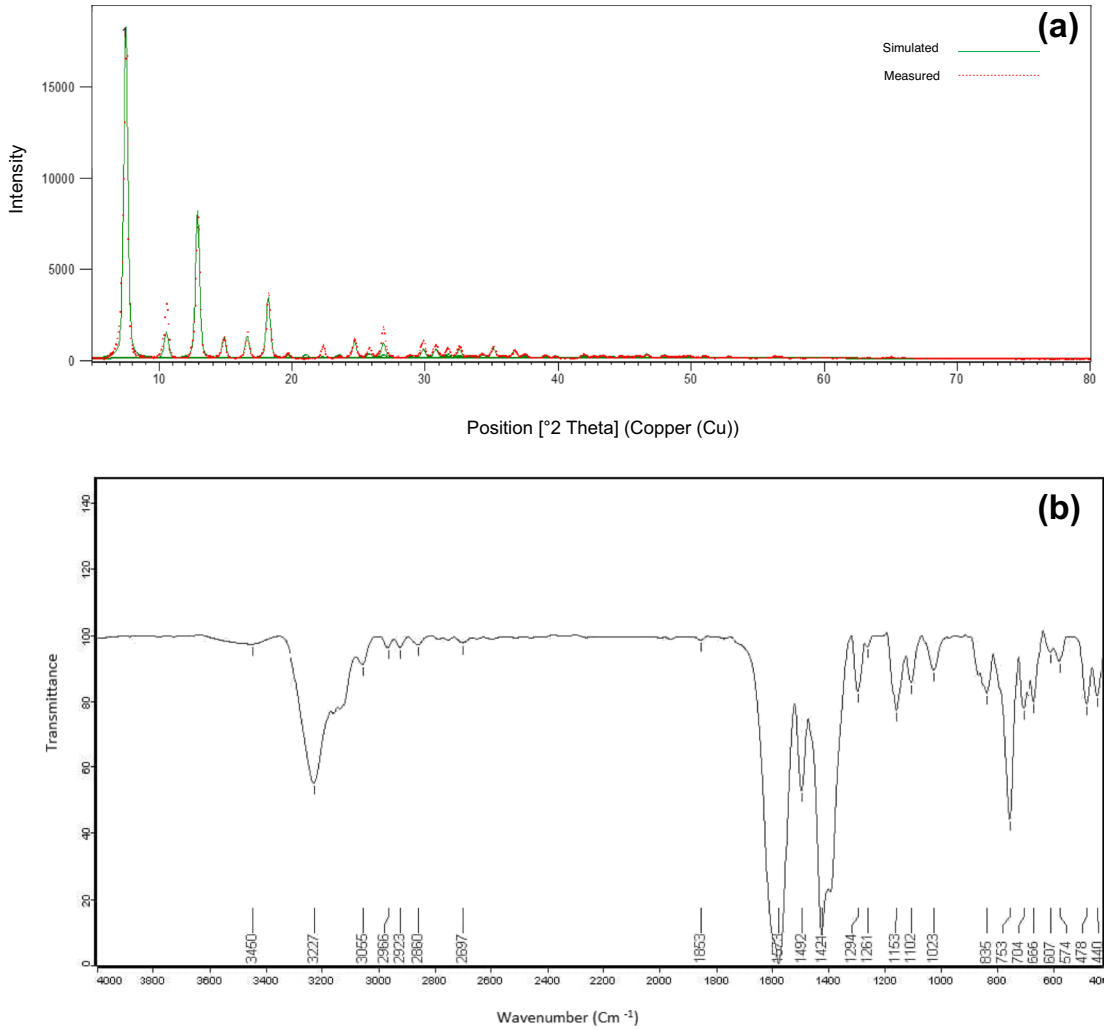

Fig. 1 (**a**) XRD pattern along with the simulated pattern using Rietveld refinement, and (**b**) FT-IR spectrum obtained from the synthesized ZIF-8 powder

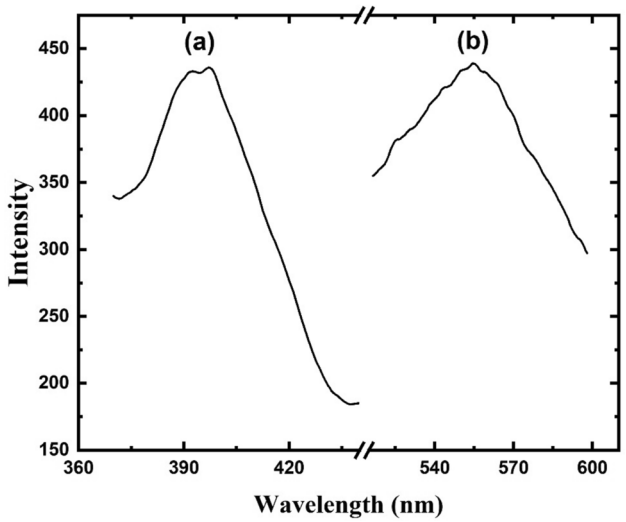

Fig. 2 (**a**) Excitation spectrum, and (**b**) fluorescence emission spectrum of ZIF-8(a)

molecules on the surface of ZIF-8 or on the solvent coating may be responsible for the peak shift in ZIF-8(a).

Luminescence Selectivity Results of Different Cations

Figure 3(a) shows luminescence spectra recorded at $\lambda_{ex} = 396$ nm for ZIF-8(a) mixed with different cations. Moreover, the corresponding luminescence intensity extracted from each spectrum is shown in Fig. 3(b) as a bar graph. As can be inferred from Fig. 3, while Fe^{3+} ion remarkably quenches the luminescence intensity of ZIF-8(a), the rest of the cations do not considerably decrease it.

Calibration Curve of Fe3+ Ion

By varying the concentration of Fe^{3+} ion, sensitivity of ZIF-8(a) was examined in order to obtain the corresponding

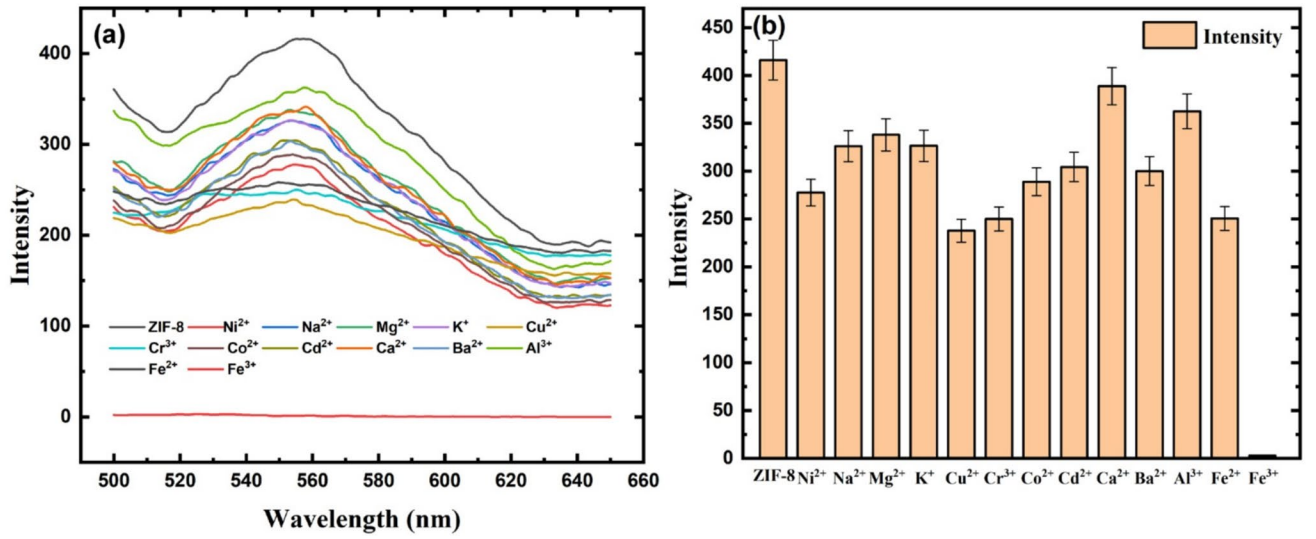

Fig. 3 (**a**) Luminescence emission spectra, and (**b**) corresponding intensity (as a bar graph) recorded at $\lambda_{ex} = 396$ nm for ZIF-8(a) mixed with different metal cations

calibration curve. To this end, 3.0 ml of ZIF-8(a) was combined with 3.0 ml of 1.0×10^{-3}–1.0×10^{-7} M solution of $Fe(NO_3)_3$. Subsequently, several experiments were performed to detect the metal ions through monitoring the behavior of fluorescence quenching of ZIF-8(a). The limit of detection (LOD) was calculated based on the following equation: LOD = 3δ/k, where k represents the calibration curve slope, and δ denotes the blank standard deviation. Accordingly, the LOD is found to be 2.1×10^{-6} M in the linear range of 1.0×10^{-4}–1.0×10^{-7} M (see Fig. 4), indicating that ZIF-8(a) has the potential to be a highly sensitive and selective fluorescence sensor for the detection of Fe^{3+} ions. It should be noted that the complete fluorescence quenching is achieved using Fe^{3+} ion concentrations higher than 1.0×10^{-4} M. Also, at concentrations below the detection limit, the calibration curve becomes non-linear.

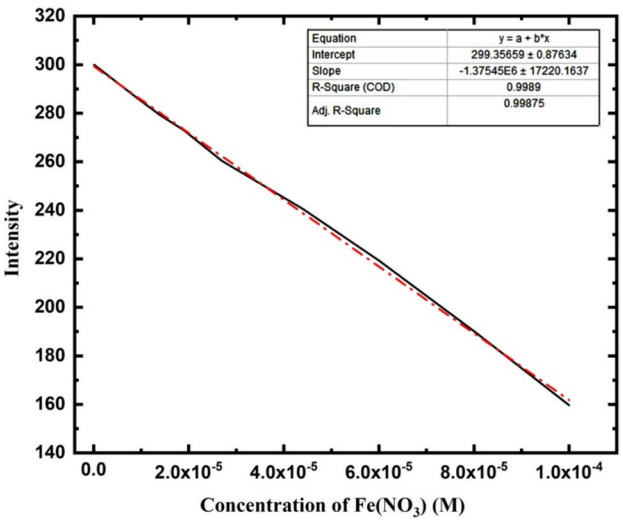

Fig. 4 Calibration curve of Fe^{3+} ion using ZIF-8(a) combined with different concentrations of $Fe(NO_3)_3$

Anti-Interference Performance of ZIF-8(a) in Detection of Fe3+ Ion

$M(NO_3)_X$ solutions (M = Al^{3+}, Cr^{3+}, Fe^{3+}, Ni^{2+}, Fe^{2+}, Co^{2+}, Mg^{2+}, Cd^{2+}, Ca^{2+}, Mn^{2+}, Na^{+}, and K^{+}) with a concentration of 0.01 M were prepared in order to examine the anti-interference performance of ZIF-8(a) in the detection of a trace amount of Fe^{3+} ion.

In this respect, ZIF-8(a) and $Fe(NO_3)_3$ were added to each metal cation solution in a ratio of 1:1:1. Therefore, the anti-interference performance of ZIF-8(a) was evaluated by studying its quenching process in the presence of other cations mixed with Fe^{3+} ion using luminescence spectra [6]. The corresponding intensity values obtained from the luminescence spectra are shown in Fig. 5 as bar graphs. As can be seen, the other cations cannot interfere with the determination of Fe^{3+} ion through quenching the fluorescence emission of ZIF-8(a). For example, in the absence of Fe^{3+} ion, Cu^{2+} cation exhibits emission, and Fe^{3+} quenches the emission when it combines with Cu^{2+} cation. It is noteworthy that, in the absence of Fe^{3+} ion, the other cations show emission, and Fe^{3+} ion quenches their emission, which indicates that there is no interference in the quenching process of Fe^{3+} ion. Therefore, ZIF-8(a) has a high degree of selectivity for Fe^{3+} ion.

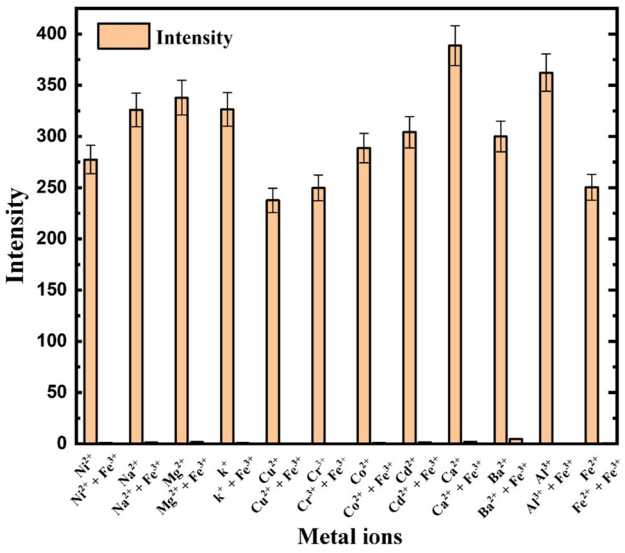

Fig. 5 The anti-interference performance of ZIF-8(a) in the presence of other cations mixed with Fe^{3+} ion using luminescence spectra. The corresponding intensity values obtained from the spectra are shown as bar graphs

Luminescence Selectivity Results of Different Anions

Similar to the cation-selective assay, luminescence selectivity of ZIF-8(a) in the detection of different anions ($Cr_2O_7^{2-}$, CrO_4^{2-}, IO_3^-, SO_4^{2-}, Br^-, Cl^-, ClO_4^-, and NO_3^-(was investigated, and the results are shown in Fig. 6. As observed, while both $Cr_2O_7^{2-}$ and CrO_4^{2-} anions quench the luminescence intensity of ZIF-8(a), the other anions do not significantly reduce it.

Calibration Curve of Cr6+ Ion

The concentration of Cr^{6+} ion was changed in order to evaluate the sensitivity of ZIF-8(a), and to obtain the corresponding calibration curve. In this regard, 3.0 ml of ZIF-8(a) was initially combined with 3.0 ml of 1×10^{-3}–1×10^{-7} M solution of $K_2Cr_2O_7$, and the ion detection was then performed through monitoring the behavior of fluorescence quenching of ZIF-8(a), according to Fig. 7. In this case, the LOD is calculated to be 7.6×10^{-7} M in the linear range of 4.7×10^{-5}–1.9×10^{-6} M, proposing ZIF-8(a) as a very good fluorescence sensor for the detection of Cr^{6+} ions. Moreover, the complete fluorescence quenching is obtained using Cr^{6+} ion concentrations higher than 4.7×10^{-5} M. At concentrations below the detection limit, the calibration curve becomes non-linear.

Anti-Interference Performance of ZIF-8(a) in Detection of Cr6+ Ion

$K_X(A)$ solutions ($A = Cr_2O_7^{2-}$, CrO_4^{2-}, IO_3^-, SO_4^{2-}, Br^-, Cl^-, ClO_4^-, NO_3^-) with a concentration of 0.01 M were prepared in order to examine the anti-interference performance of ZIF-8(a) in the detection of a trace amount of Cr^{6+} ion. To this end, ZIF-8(a) and $K_2Cr_2O_7$ were added to each metal anion solution in a ratio of 1:1:1, followed by evaluating the quenching process of ZIF-8(a) in the presence of other anions mixed with Cr^{6+} ion using luminescence spectra [8]. Figure 8 shows the corresponding intensity values obtained from the luminescence spectra as bar graphs. As viewed, the other anions are not able to interfere with the determination of Cr^{6+} ion through quenching the fluorescence emission of ZIF-8(a), indicating a high degree of selectivity for Cr^{6+} ion.

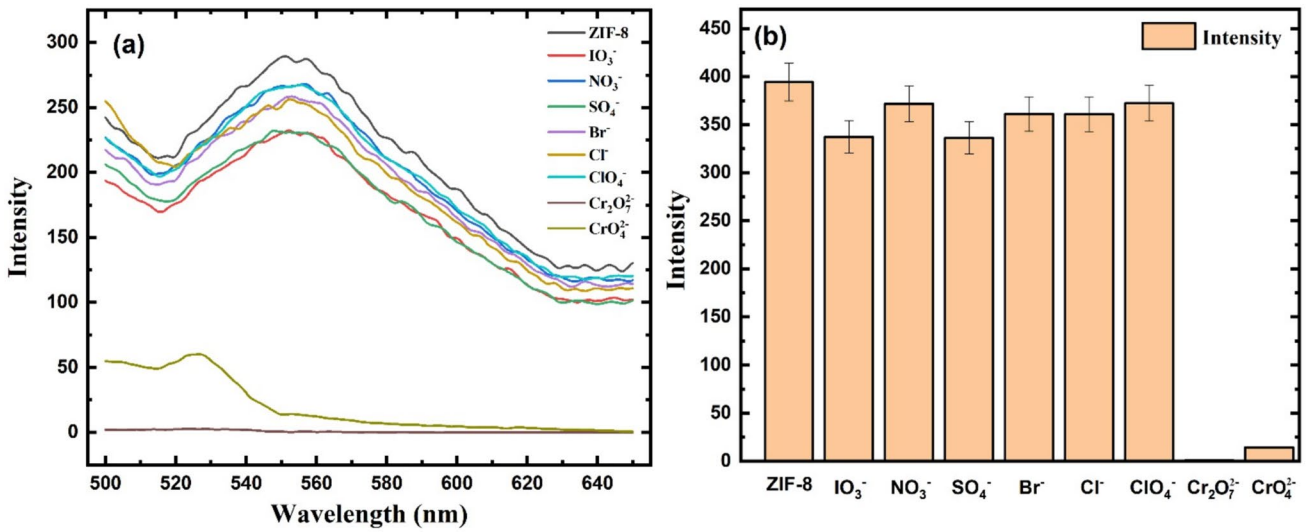

Fig. 6 (**a**) Luminescence emission spectra, and (**b**) corresponding intensity (as a bar graph) recorded at $\lambda_{ex} = 396$ nm for ZIF-8(a) mixed with different metal anions

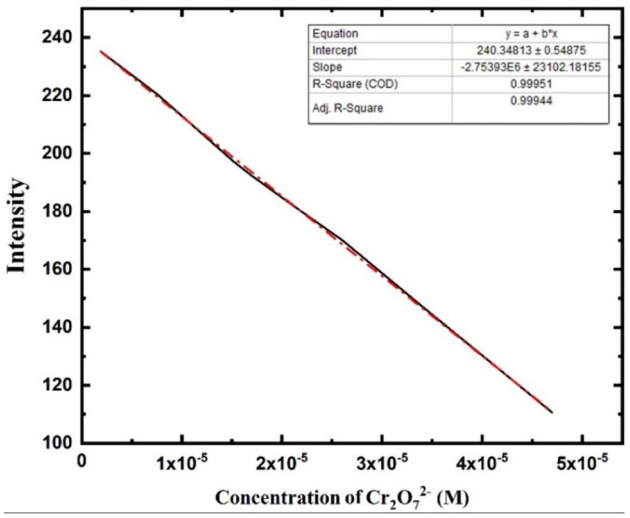

Fig. 7 Calibration curve of Cr^{6+} ion using ZIF-8(a) combined with different concentrations of $Cr_2O_7^{2-}$

In order to compare the performance of the pure ZIF-8(a) sensor in this study with that of ZIF-based sensors in the literature, the target metal ions (mainly Fe^{3+} and Cr^{6+}), LOD and limit of linearity (LOL) for these materials are presented in Table 1. As inferred, the LOD of the pure ZIF-8(a) is significantly lower than that of ZIF-based materials reported in previous studies. Also, Table 2 presents the comparison between metal ion detection performances of the pure ZIF-8(a) and MOF and coordination polymers developed for the detection of Fe^{3+} and Cr^{6+} ions, indicating the lower LOD

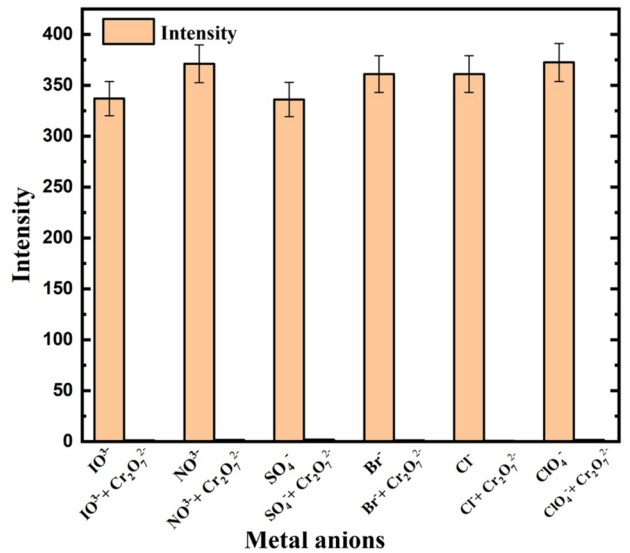

Fig. 8 The anti-interference performance of ZIF-8(a) in the presence of other anions mixed with Cr^{6+} ion using luminescence spectra. The corresponding intensity values obtained from the spectra are shown as bar graphs

of the pure ZIF-8(a). In addition to the lower LOD compared to other MOFs, the lower synthesis cost of ZIF-8(a) and its ease of preparation are noteworthy. In fact, detecting Fe^{3+} and Cr^{6+} ions was possible without changing the main structure of the ZIF-8 framework.

Fluorescence Quenching Mechanism

Normally, the following possible phenomena are involved in the fluorescence quenching mechanism: framework collapse, ion exchange, competitive absorption of excited light or resonance energy transfer, and some specific interactions occurring between the MOF and analyte [10, 36, 45]. Here, the quenching mechanism of ZIF-8(a) was studied using XRD patterns. For this purpose, ZIF-8(a) was immersed in the analyte solutions (Fe^{3+} and Cr^{6+}) for one day, while also performing XRD analysis after the immersion. The results obtained are shown in Fig. 9. As seen in Fig. 9(a), by immersing ZIF-8(a) in 0.01 M $K_2Cr_2O_7$ solution, the crystal structure of ZIF-8 is completely destroyed or becomes amorphous. Therefore, the mechanism of ZIF-8(a) luminescence quenching by Cr^{6+} ion is due to the collapse of the main framework structure.

In the case of ZIF-8(a) immersed in 0.01 M Fe^{3+} solution, the XRD pattern depicted in Fig. 9(b) shows the appearance of some peaks related to the ZIF-8. Thus, the crystal structure of ZIF-8(a) is not entirely destroyed after immersing it in the Fe^{3+} solution. In other words, the fluorescence quenching mechanism of ZIF-8(a) by Fe^{3+} ions may not be dominated by the collapse of the main framework structure. The difference in the behavior of Cr^{6+} and Fe^{3+} ions against ZIF-8 can be related to their different chemical nature, ionic radius ($r_{Cr}{}^{6+} = 0.54$ Å and $r_{Fe}{}^{3+} = 0.63$ Å) and electrical charge, as well as their chemical reactions with the ZIF-8 structure. Therefore,

Table 1 The comparison between metal ion detection performances of the pure ZIF-8(a) in this study and ZIF-based materials reported in the literature

Material	Target metal ion	LOD	LOL	Ref
R6G@ZIF-8	Fe^{3+}, Cr^{6+}: MnO_4^- CrO_4^{2} $Cr_2O_7^{2-}$ and aniline	5 μM 50 μM 5 Mm	–	[2]
CdTe QD@ ZIF-8	Cu^{2+} Fe^{2+}	1.45 μM 0.29 μM	1–50 μM 1–60 μM	[14]
ZIF-8@Ma	Fe^{3+}	1.17 μM	0.001–10 μM	[15]
Ag/Zn@ZIF-8	Fe^{3+} Cu^{2+}	3.9 μM 6.7 μM	1–10 μM 1–10 μM	[37]
ZIF-8	Fe^{3+} Cr^{6+} ($Cr_2O_7^{2}$)	2.1 μM 0.76 μM	0.1–100.0 μM 1.9–47.0 μM	This study

Table 2 The comparison between metal ion detection performances of the pure ZIF-8(a) in this study and MOF and coordination polymers for the detection of Fe^{3+} and Cr^{6+} ions reported in the literature

Material	Target metal ion	LOD	Ref
$[Zn_3(OH)_2(btca)2{\cdot}2DMF]{\cdot}H_2O$ (1)	Fe^{3+} Cr^{6+} Cr^{3+}	9.87×10^{-6} M 9.56×10^{-6} M 9.31×10^{-6} M	[1]
IISERP-MOF25	Fe^{3+}	3.6 ppm	[3]
$\{[Zn_2(\mu_3\text{-}OH)(cpta)(4,4'\text{-}bipy)]{\cdot}H_2O\}n$ (1)	$Cr_2O_7^{2-}$ Cr^{3+}	6.91×10^{-6} M 5.55×10^{-6} M	[6]
$\{[Cd(CIP)_2(H_2O)2]n{\cdot}2.5H_2O\}$ (1)	Fe^{3+} CrO_4^{2-} $Cr_2O_7^{2}$	4.69×10^{4} M^{-1} 3.99×10^{4} M^{-1} 3.45×10^{4} M^{-1}	[39]
$[Cd(Hcbic)]_n$	Fe^{3+}	3.1×10^{-5} M	[40]
{[Zn(L)(bpp)•DMF}n	Fe^{3+} $Cr_2O_7^{2-}$	1.55×10^{-6} M 3.52×10^{-6} M	[41]
$[Ln(\mu_3\text{-cpta})(phen)(H_2O)_2]_n$	Fe^{3+}	2×10^{-4} M	[42]
HPU-1 (Zn)	Fe^{3+}	1.09×10^{-3} M	[43]
SUMOF-7II	Fe^{3+}	1.66×10^{-5} M	[44]
ZIF-8	Fe^{3+} Cr^{6+} ($Cr_2O_7^{2-}$)	2.1 μM 0.76 μM	This study

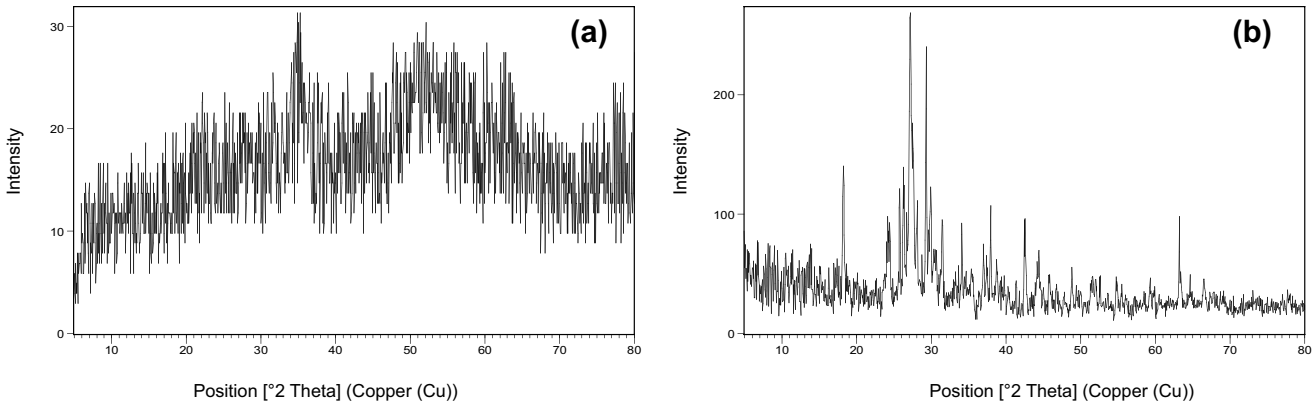

Fig. 9 XRD patterns obtained from ZIF-8(a) after immersion in: (**a**) Cr^{6+} and (**b**) Fe^{3} solutions

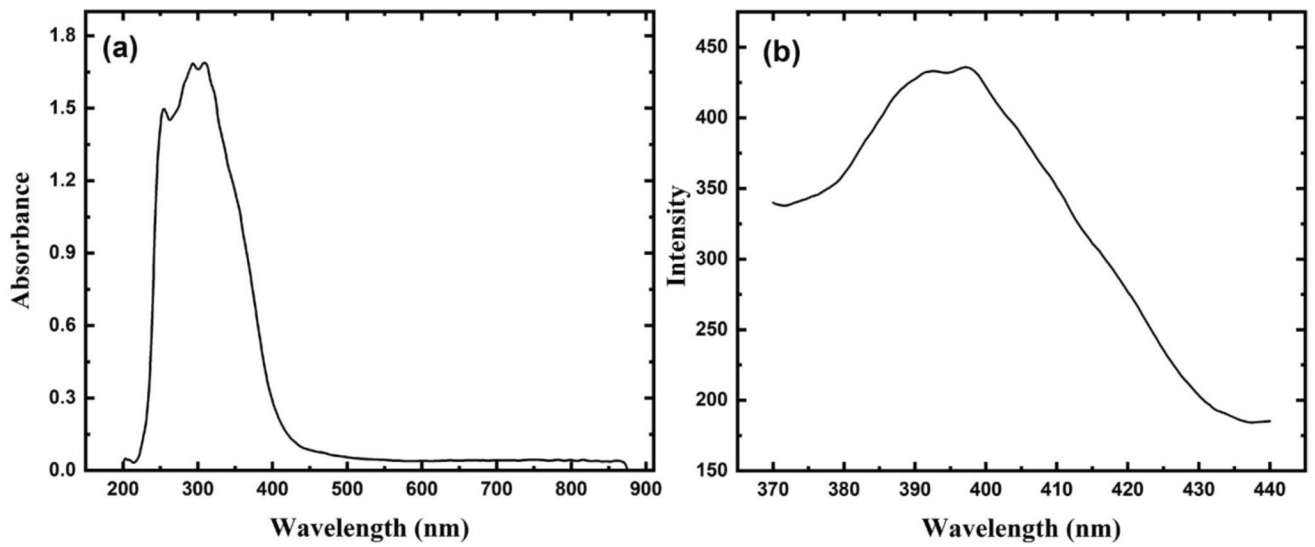

Fig. 10 (**a**) UV–vis spectrum of Fe^{3+} ion, and (**b**) excitation spectrum of ZIF-8(a)

the Cr^{6+} ion can easily penetrate the ZIF-8 and break the bonds, leading to collapse of the structure.

It should be noted that, under suitable conditions such as neutral pH and ambient temperature, it was possible to use the ZIF-8 in an aqueous environment for up to 4 weeks without changing the fluorescence intensity.

The resonance energy transfer was investigated to study the quenching mechanism using UV–vis spectroscopy. Generally, when the analyte's absorption spectrum partially overlaps with the emission or excitation spectrum of MOF, a competitive energy absorption can occur between the MOF and analyte, leading to the absorbance of energy by the acceptor and causing the fluorescence quenching [1, 16, 46].

The UV–vis spectrum of Fe^{3+} ion and the excitation spectrum of ZIF-8(a) are depicted in Fig. 10(a) and (b), respectively. Given that ZIF-8(a) and Fe^{3+} ion have strong excitation bands in the wavelength ranges of 360–420 nm and 200–420 nm, respectively, the absorption spectrum of the analyte is found to overlap with the excitation spectrum of MOF, indicating that the emission quenching of ZIF-8(a) is caused by the resonance energy transfer. On the other hand, an electron transfer from donor to acceptor may be responsible for the quenching effect of Fe^{3+} ion, as demonstrated in several studies in the literature [12, 20].

In fact, the imidazole rings of ZIF-8 are considered good electron donors when excited by light. Also, Fe^{3+} ions have high positive charge density, inducing large electron withdrawing affinity compared to other metal ions [5]. In this way, Fe^{3+} ions can accept electrons from them to form coordination interactions. Consequently, the energy migration occurs when electrons are transferred from the donor to the acceptor (from electron rich ligand to the Fe^{3+} ion), resulting in the quenching of luminescence [5, 20].

Conclusion

A chemical method has been utilized to synthesize ZIF-8, acting as a fluorescent sensor in the detection of trace amounts of Fe^{3+} and Cr^{6+} ions dissolved in water. XRD and FT-IR analyses indicated high purity and sodalite structure of the synthesized ZIF-8. The maximum emission intensity of the ZIF-8 was observed at $\lambda_{ex} = 396$ and 555 nm, revealing a peak shift due to the introduction of water into the highly crystalline structure of ZIF-8. Both Fe^{3+} and Cr^{6+} ions remarkably quenched the luminescence intensity of ZIF-8, giving rise to LODs of 2.1 and 0.76 µM, respectively. Meanwhile, the corresponding LOLs were calculated to be 0.1–100.0 and 1.9–47.0 µM, outperforming the detection performance of ZIF-based, MOF and coordination polymer materials reported in previous studies (see Tables 1 and 2). The quenching mechanism of the ZIF-8 was also studied in detail, indicating that the resonance energy transfer and collapse of ZIF-8 main framework were responsible for the quenching effects of Fe^{3+} and Cr^{6+} ions, respectively. Overall, the pure ZIF-8 with the high degree of selectivity of the metal ions can be considered an efficient fluorescence sensor, providing a possible alternative tool to more sophisticated methods such as ICP, ICP-MS, HPLC, etc.

Supplementary Information The online version contains supplementary material available at https://doi.org/10.1007/s10895-025-04259-1.

Acknowledgements I acknowledge the University of Kashan for supporting of the work.

Author Contribution Fariba Erfani is a Ph.D. student and write the manuscript. Ali Ghlami and Sayed Mehdi Ghoreishi are supervisors. SMG reviewed the manuscript.

Funding None.

Data Availability No datasets were generated or analysed during the current study.

Declarations

Conflicts of Interest The authors declare no competing interests.

References

1. Liu H, Ma Z, Meng F, Ding Y, Fu Y, Zheng M, Yang J (2022) A Water-Stable Zinc (II)-Organic framework for selective sensing of Fe^{3+} and Cr^{6+} ions. Polyhedron 222:115930. https://doi.org/10.1016/j.poly.2022.115930
2. Han T, Yang J, Liu Y, Ma F (2016) Rhodamine 6G loaded zeolitic imidazolate framework-8 (ZIF-8) nanocomposites for highly selective luminescent sensing of Fe^{3+}, Cr^{6+} and aniline. Microporous Mesoporous Mater 228:275–288. https://doi.org/10.1016/j.micromeso.2016.04.005
3. Maity R, Chakraborty D, Nandi S, Yadav K, Mullangi D, Vinod P, Vaidhyanathan R (2019) Aqueous-phase differentiation and speciation of Fe^{3+} and Fe^{2+} using water-stable photoluminescent lanthanide-based metal–organic framework. ACS Appl Nano Mater 2(8):5169–5178. https://doi.org/10.1021/acsanm.9b01047
4. Liu W, Xie J, Zhang L, Silver A, Wang S (2018) A hydrolytically stable uranyl organic framework for highly sensitive and selective detection of Fe^{3+} in aqueous media. Dalton Trans 47(3):649–653. https://doi.org/10.1039/C7DT04365A
5. Fajal S, Samanta P, Dutta S, Ghosh K (2020) Selective and sensitive recognition of Fe^{3+} ion by a Lewis basic functionalized chemically stable metal-organic framework (MOF). Inorg Chim Acta 502:119359. https://doi.org/10.1016/j.ica.2019.119359
6. Wang J, Fan Y, Lee W, Yi C, Cheng C, Zhao X, Yang M (2018) Ultrasmall metal–organic framework Zn-MOF-74 nanodots: size-controlled synthesis and application for highly selective colorimetric sensing of iron (III) in aqueous solution. ACS Appl Nano Mater 1(7):3747–3753. https://doi.org/10.1021/acsanm.8b01083
7. Ge Y, Sun GH, Meng L, Ren S, Zheng G (2019) Four new luminescent metal–organic Frameworks as multifunctional sensors for detecting Fe^{3+}, $Cr_2O_7^{2-}$ and nitromethane. Cryst Growth Des 20(3):1898–1904. https://doi.org/10.1021/acs.cgd.9b01593
8. Valadi M, Shahsavari S, Akbarzadeh E, Gholami R (2022) Preparation of new MOF-808/chitosan composite for Cr (VI) adsorption from aqueous solution: Experimental and DFT study. Carbohyd Polym 288:119383. https://doi.org/10.1016/j.carbpol.2022.119383

9. Jin H, Xu J, Zhang L, Ma B, Shi X, Fan Y, Wang L (2018) Multi-responsive luminescent sensor based on Zn (II) metal-organic framework for selective sensing of Cr (III), Cr (VI) ions and p-nitrotolune. J Solid State Chem 268:168–174. https://doi.org/10.1016/j.jssc.2018.08.035
10. Yang S, Chen S, Li K, Luo Q, Zhang Y, Wang L, Wu S, Zhu M (2023) A water-stable metal–organic framework Zn-MOF as a chemical sensor for efficient detection of Cr (VI) ($Cr_2O_7^{2-}$and CrO_4^{2-}) anions in water. Inorg Chim Acta 558:121764. https://doi.org/10.1016/j.ica.2023.121764
11. Mandal W, Fajal S, Desai V, Ghosh K (2025) Metal-organic frameworks (MOFs) and related other advanced porous materials for sequestration of heavy metal-based toxic oxo-pollutants from water. Coord Chem Rev 524:216326. https://doi.org/10.1016/j.ccr.2024.216326
12. Xiang Z, Fang C, Leng S, Cao D (2014) An amino group functionalized metal–organic framework as a luminescent probe for highly selective sensing of Fe^{3+} ions. J Mater Chem A 2(21):7662–7665. https://doi.org/10.1039/C4TA00313F
13. Zhang A, Fan C, Sun W, Chen L, Shi R, Cao Y, Yang P (2019) Cu^{2+} and Fe^{2+} sensor based on CdTe QD@ZIF-8 composites. J Nanosci Nanotechnol 19(12):8088–8094. https://doi.org/10.1166/jnn.2019.16756
14. Wang Y, Zhang Y, Liao H, Yin B, Zhao Y, Gao N, Jiang H, Mao R, Yang X (2022) Multi-responsive luminescent MOF sensor for Fe^{3+}, CrO_4^{2-} and $Cr_2O_7^{2-}$ in aqueous solution based on phenylenediacetate and bis-imidazole ligand. J Mol Struct 1264:133239. https://doi.org/10.1016/j.molstruc.2022.133239
15. Zhang S, Liu Y, Yu L, Wang H, Xu Y, Zhao Y (2022) A highly selective and fast-response fluorescent sensor based on a composite material ZIF-8@ MA for the detection of trace amounts of Fe^{3+} ion. J Mol Struct 1262:133076. https://doi.org/10.1016/j.molstruc.2022.133076
16. Lv R, Li H, Su J, Fu X, Yang B, Gu W, Liu X (2017) Zinc metal–organic framework for selective detection and differentiation of Fe (III) and Cr (VI) ions in aqueous solution. Inorg Chem 56(20):12348–12356. https://doi.org/10.1021/acs.inorgchem.7b01822
17. Mandal W, Fajal S, Samanta P, Dutta S, Shirolkar MD, Ghosh K (2022) Selective and sensitive recognition of specific types of toxic organic pollutants with a chemically stable highly luminescent porous organic polymer (POP). ACS Appl Polym Mater 4(11):8633–8644. https://doi.org/10.1021/acsapm.2c01538
18. Fajal S, Mandal W, Majumder D, Shirolkar M, More D, Ghosh K (2022) Unfolding the Role of Building Units of MOFs with Mechanistic Insight Towards Selective Metal Ions Detection in Water. Chem–A Eur J 28(21): e202104175.
19. Ma X-L, Lin JYS (2017) Preparation chemistry of inorganic membranes. In: Modern inorganic synthetic chemistry, 2nd edn. Elsevier, pp 669–686. https://doi.org/10.1016/B978-0-444-63591-4.00023-9
20. Han T, Bai L, Liu Y, Ma F (2019) Two host-guest hybrids by encapsulation AlQ3 in zeolitic imidazolate framework-8 as luminescent sensors for Fe^{3+}, $CrO_4^{2-}$and acetone. J Solid State Chem 269:588–593. https://doi.org/10.1016/j.jssc.2018.10.044
21. Zhou H, Li L, Li H, Li A, Yang T, Huang W (2013) A flexible Eu (III)-based metal–organic framework: turn-off luminescent sensor for the detection of Fe (III) and picric acid. Dalton Trans 42(34):12403–12409. https://doi.org/10.1039/C3DT51081F
22. Lin X, Hong Y, Zhang C, Huang R, Wang C, Lin W (2015) Preconcentration and energy transfer enable the efficient luminescence sensing of transition metal ions by metal–organic frameworks. Chem Commun 51(95):16996–16999. https://doi.org/10.1039/C5CC06453H
23. Xu Y, Yan B (2015) Eu (III)-functionalized MIL-124 as fluorescent probe for highly selectively sensing ions and organic small molecules especially for Fe (III) and Fe (II). ACS Appl Mater Interfaces 7(1):721–729. https://doi.org/10.1021/am5070409
24. Wen X, Han L, Wu Q, Wu P, Dong W, Zhao J, Li Sh, Ma F (2016) A multi-responsive luminescent sensor based on a super-stable sandwich-type terbium (III)–organic framework. Dalton Trans 45(39):15492–15499. https://doi.org/10.1039/C6DT03057B
25. Parmar B, Rachuri Y, Bisht K, Suresh E (2017) Mixed-ligand LMOF fluorosensors for detection of Cr (VI) oxyanions and Fe^{3+}/Pd^{2+} cations in aqueous media. Inorg Chem 56(18):10939–10949. https://doi.org/10.1021/acs.inorgchem.7b01130
26. Pal S, Bharadwaj PK (2016) A luminescent terbium MOF containing hydroxyl groups exhibits selective sensing of nitroaromatic compounds and Fe (III) ions. Cryst Growth Des 16(10):5852–5858. https://doi.org/10.1021/acs.cgd.6b00930
27. Wang R, Liu X, Huang A, Wang W, Xiao Z, Zhang L, Dai F, Sun D (2016) Unprecedented solvent-dependent sensitivities in highly efficient detection of metal ions and nitroaromatic compounds by a fluorescent barium metal–organic framework. Inorg Chem 55(4):1782–1787. https://doi.org/10.1021/acs.inorgchem.5b02693
28. Zhao L, Tian D, Gao Q, Sun W, Xu J, Bu H (2016) A chiral lanthanide metal–organic framework for selective sensing of Fe (III) ions. Dalton Trans 45(3):1040–1046. https://doi.org/10.1039/C5DT03283K
29. Zhang Y, Jia Y, Li M, Hou A (2018) Influence of the 2-methylimidazole/zinc nitrate hexahydrate molar ratio on the synthesis of zeolitic imidazolate framework-8 crystals at room temperature. Sci Rep 8(1):9597. https://doi.org/10.1038/s41598-018-28015-7
30. Wang Y, Dai X, Zhan Y, Ding X, Wang M, Wang X (2019) In situ growth of ZIF-8 nanoparticles on chitosan to form the hybrid nanocomposites for high-efficiency removal of Congo Red. Int J Biol Macromol 137:77–86. https://doi.org/10.1016/j.ijbiomac.2019.06.195
31. Pillai P, Dharaskar S, Sasikumar S, Khalid M (2019) Zeolitic imidazolate framework-8 nanoparticle: a promising adsorbent for effective fluoride removal from aqueous solution. Appl Water Sci 9:1–12. https://doi.org/10.1007/s13201-019-1030-9
32. Zhang Y, Jia Y (2018) Synthesis of zeolitic imidazolate framework-8 on polyester fiber for PM 2.5 removal. RSC Adv 8(55): 31471–31477. https://doi.org/10.1039/C8RA06414H
33. Olga K, Marianne L, Wojciech B, Amy S, Omar a, Joseph H, (2012) A Catalytically Active Zeolitic Imidazolate Framework of Sodalite Topology with Unsubstituted Linkers. J Am Chem Soc 134:18790–18796. https://doi.org/10.1021/ja308786r
34. Niknam M, Ghahramaninezhad M, Eydifarash M (2017) Zeolitic imidazolate framework-8 for efficient adsorption and removal of Cr (VI) ions from aqueous solution. Environ Sci Pollut Res 24:9624–9634. https://doi.org/10.1007/s11356-017-8577-5
35. Siva V, Murugan A, Shameem A, Thangarasu S, Bahadur A (2022) A simple synthesis method of zeolitic imidazolate framework-8 (ZIF-8) nanocrystals as superior electrode material for energy storage systems. J Inorg Organomet Polym Mater 32(12):4707–4714. https://doi.org/10.1007/s10904-022-02475-x
36. Geng R, Tang H, Ma Q, Liu L, Feng W, Zhang Z (2022) Bimetallic Ag/Zn-ZIF-8: An efficient and sensitive probe for Fe^{3+} and Cu^{2+} detection. Colloids Surf, A 632:127755. https://doi.org/10.1016/j.colsurfa.2021.127755
37. Liu S, Xiang Z, Hu Z, Zheng X, Cao D (2011) Zeolitic imidazolate framework-8 as a luminescent material for the sensing of metal ions and small molecules. J Mater Chem 21(18):6649–6653. https://doi.org/10.1039/C1JM10166H
38. Yang X, Yan D (2017) Direct white-light-emitting and near-infrared phosphorescence of zeolitic imidazolate framework-8. Chem Commun 53(11):1801–1804. https://doi.org/10.1039/C6CC09706E
39. Wang Q, Feng D, Zhao D, Fang D, Tang J, Fan M, Yang J (2019) A multifunctional 1D Cd-based metal-organic complex for the highly luminescent sensitive detection of Fe^{3+}, CrO_4^{2-}/$Cr_2O_7^{2-}$, and nitroaromatic explosives. J Solid State Chem 274:40–46. https://doi.org/10.1016/j.jssc.2019.02.013

40. Li F, Zhu L, Lu P (2018) A luminescent Cd (II)-based metal− organic framework for detection of Fe (III) ions in aqueous solution. J Solid State Chem 261:31–36. https://doi.org/10.1016/j.jssc.2018.02.006
41. Chen Z, Mi X, Wang S, Lu J, Li Y, Li D, Dou J (2018) Two novel penetrating coordination polymers based on flexible S-containing dicarboxylate acid with sensing properties towards Fe^{3+} and $Cr_2O_7^{2-}$ions. J Solid State Chem 261:75–85. https://doi.org/10.1016/j.jssc.2018.02.008
42. Gu Z, Cai Y, Liu Y, Liang X, Kirillov M (2018) New lanthanide 2D coordination polymers constructed from a flexible ether-bridged tricarboxylate block: Synthesis, structures and luminescence sensing. Inorg Chim Acta 469:98–104. https://doi.org/10.1016/j.ica.2017.08.054
43. Li H, He Y, Li Q, Li S, Yi Z, Xu Z, Wang Y (2017) Highly sensitive and selective fluorescent probe for Fe^{3+} and hazardous phenol compounds based on a water-stable Zn-based metal–organic framework in aqueous media. RSC Adv 7(79):50035–50039. https://doi.org/10.1039/C7RA08427G
44. Abdelhamid N, Bermejo-Gómez A, Martín-Matute B, Zou X (2017) A water-stable lanthanide metal-organic framework for fluorimetric detection of ferric ions and tryptophan. Microchim Acta 184:3363–3371. https://doi.org/10.1007/s00604-017-2306-0
45. Xiao Y, Cui Y, Zheng Q, Xiang S, Qian G, Chen B (2010) A microporous luminescent metal–organic framework for highly selective and sensitive sensing of Cu^{2+} in aqueous solution. Chem Commun 46(30):5503–5505. https://doi.org/10.1039/C0CC00148A
46. Diamantis A, Margariti A, Pournara D, Papaefstathiou S, Manos J, Lazarides T (2018) Luminescent metal–organic frameworks as chemical sensors: common pitfalls and proposed best practices. Inorg Chem Front 5(7):1493–1511. https://doi.org/10.1039/C8QI00090E